
RESONATOR OPTICS

9.1 PLANAR-MIRROR RESONATORS

- A. Resonator Modes
- B. The Resonator as a Spectrum Analyzer
- C. Two- and Three-Dimensional Resonators

9.2 SPHERICAL-MIRROR RESONATORS

- A. Ray Confinement
- B. Gaussian Modes
- C. Resonance Frequencies
- D. Hermite – Gaussian Modes
- *E. Finite Apertures and Diffraction Loss



Charles Fabry (1867–1945)



Alfred Perot (1863–1925)

Fabry and Perot constructed an optical resonator for use as an interferometer. Now known as the Fabry–Perot etalon, it is used extensively in lasers.

An optical resonator, the optical counterpart of an electronic resonant circuit, confines and stores light at certain resonance frequencies. It may be viewed as an optical transmission system incorporating feedback; light circulates or is repeatedly reflected within the system, without escaping. The simplest resonator comprises two parallel planar mirrors between which light is repeatedly reflected with little loss. Typical optical resonator configurations are depicted in Fig. 9.0-1.

The frequency selectivity of an optical resonator makes it useful as an optical filter or spectrum analyzer. Its most important use, however, is as a “container” within which laser light is generated. The laser is an optical resonator containing a medium that amplifies light. The resonator determines the frequency and spatial distribution of the laser beam. Because resonators have the capability of storing energy, they can also be used to generate pulses of laser energy. Lasers are discussed in Chap. 14; the material in this chapter is essential to their understanding.

Several approaches are useful for describing the operation of an optical resonator:

- The simplest approach is based on *ray optics* (Chap. 1). Optical rays are traced as they reflect within the resonator; the geometrical conditions under which they remain confined are determined.
- *Wave optics* (Chap. 2) is used to determine the modes of the resonator, i.e., the resonance frequencies and wavefunctions of the optical waves that exist self-consistently within the resonator. This analysis is similar to that used in Sec. 7.1 to determine the modes of a planar-mirror waveguide.

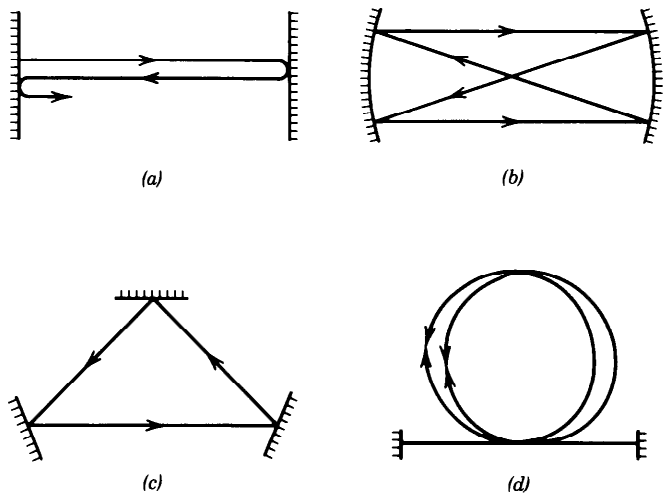


Figure 9.0-1 Optical resonators: (a) planar-mirror resonator; (b) spherical-mirror resonator; (c) ring resonator; (d) optical-fiber resonator.

- The modes of a resonator with spherical mirrors are Gaussian and Hermite–Gaussian optical beams. The study of *beam optics* (Chap. 3) is therefore useful for understanding the behavior of spherical-mirror resonators.
- *Fourier optics* and the theory of propagation and diffraction of light (Chap. 4) are necessary for understanding the effect of the finite size of the resonator's mirrors on its loss and on the spatial distribution of the modes.

The optical resonator evidently provides an excellent arena for applying the different theories of light presented in earlier chapters.

9.1 PLANAR-MIRROR RESONATORS

A. Resonator Modes

In this section we examine the modes of a resonator constructed of two parallel, highly reflective, flat mirrors separated by a distance d (Fig. 9.1-1). This simple one-dimensional resonator is known as a **Fabry–Perot etalon**. We first consider an ideal resonator whose mirrors are lossless; the effect of losses is included subsequently.

Resonator Modes as Standing Waves

A monochromatic wave of frequency ν has a wavefunction

$$u(\mathbf{r}, t) = \text{Re}\{U(\mathbf{r}) \exp(j2\pi\nu t)\},$$

which represents the transverse component of the electric field. The complex amplitude $U(\mathbf{r})$ satisfies the Helmholtz equation, $\nabla^2 U + k^2 U = 0$, where $k = 2\pi\nu/c$ is the wavenumber and c is the speed of light in the medium (see Secs. 2.2, 5.3, and 5.4). The modes of a resonator are the basic solutions of the Helmholtz equation subject to the appropriate boundary conditions. For the planar-mirror resonator, the transverse components of the electric field vanish at the surfaces of the mirrors, so that $U(\mathbf{r}) = 0$ at the planes $z = 0$ and $z = d$ in Fig. 9.1-2. The standing wave

$$U(\mathbf{r}) = A \sin kz, \tag{9.1-1}$$

where A is a constant, satisfies the Helmholtz equation and vanishes at $z = 0$ and $z = d$ if k satisfies the condition $kd = q\pi$, where q is an integer. This restricts k to

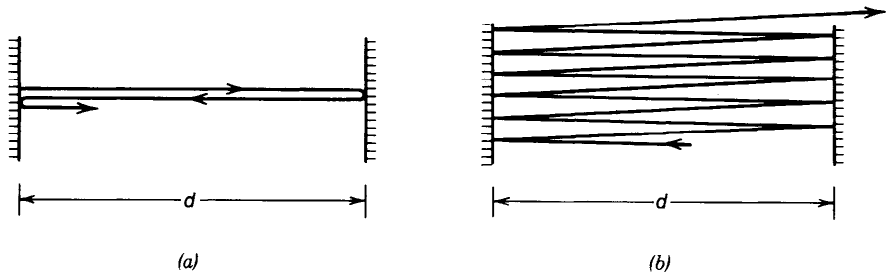


Figure 9.1-1 Two-mirror planar resonator (Fabry–Perot etalon). (a) Light rays perpendicular to the mirrors reflect back and forth without escaping. (b) Rays that are only slightly inclined eventually escape. Rays also escape if the mirrors are not perfectly parallel.

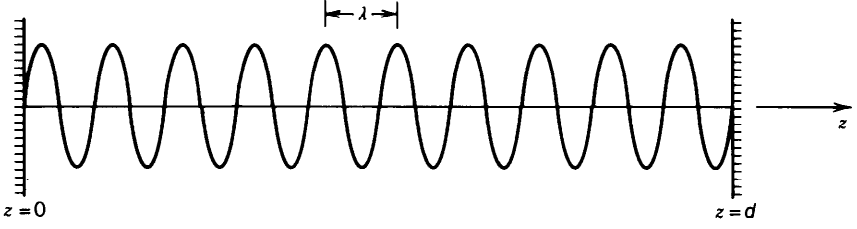


Figure 9.1-2 Complex amplitude of a resonator mode ($q = 20$).

the values

$$k_q = \frac{q\pi}{d}, \quad (9.1-2)$$

so that the modes have complex amplitudes $U(\mathbf{r}) = A_q \sin k_q z$, where the A_q are constants. Negative values of q do not constitute independent modes since $\sin k_{-q} z = -\sin k_q z$. The value $q = 0$ is associated with a mode that carries no energy since $k_0 = 0$ and $\sin k_0 z = 0$. The modes of the resonator are therefore the standing waves $A_q \sin k_q z$, where the positive integer $q = 1, 2, \dots$ is called the mode number. An arbitrary wave inside the resonator can be written as a superposition of the resonator modes, $U(\mathbf{r}) = \sum_q A_q \sin k_q z$.

It follows from (9.1-2) that the frequency $\nu = ck/2\pi$ is restricted to the discrete values

$$\nu_q = q \frac{c}{2d}, \quad q = 1, 2, \dots, \quad (9.1-3)$$

which are the resonance frequencies of the resonator. As shown in Fig. 9.1-3 adjacent resonance frequencies are separated by a constant frequency difference

$$\nu_F = \frac{c}{2d}.$$

(9.1-4)

Frequency Spacing of
Adjacent Resonator Modes

The resonance wavelengths are, of course, $\lambda_q = c/\nu_q = 2d/q$. At resonance, the length of the resonator, $d = q\lambda/2$, is an integer number of half wavelengths. Note that $c = c_0/n$ is the speed of light in the medium embedded between the two mirrors, and the λ_q represent wavelengths in the medium.

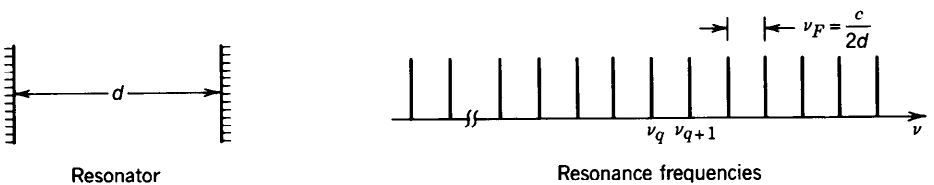


Figure 9.1-3 The resonance frequencies of a planar-mirror resonator are separated by $\nu_F = c/2d$. If the resonator is 15 cm long ($d = 15$ cm) and $n = 1$, for example, then $\nu_F = 1$ GHz.

Resonator Modes as Traveling Waves

The resonator modes can alternatively be determined by following a wave as it travels back and forth between the two mirrors [Fig. 9.1-4(a)]. A mode is a self-reproducing wave, i.e., a wave that reproduces itself after a single round trip (see Appendix C). The phase shift imparted by the two mirror reflections is 0 or 2π (π at each mirror). The phase shift imparted by a single round trip of propagation (a distance $2d$), $\varphi = k2d = 4\pi\nu d/c$, must therefore be a multiple of 2π ,

$$\varphi = k2d = q2\pi, \quad q = 1, 2, \dots \tag{9.1-5}$$

This leads to the relation $kd = q\pi$ and the resonance frequencies in (9.1-3). Equation (9.1-5) may be regarded as a condition of positive feedback in the system shown in Fig. 9.1-4(b); this requires that the output of the system be fed back *in phase* with the input.

We now show that only self-reproducing waves, or combinations thereof, can exist within the resonator in the steady state. Consider a monochromatic plane wave of

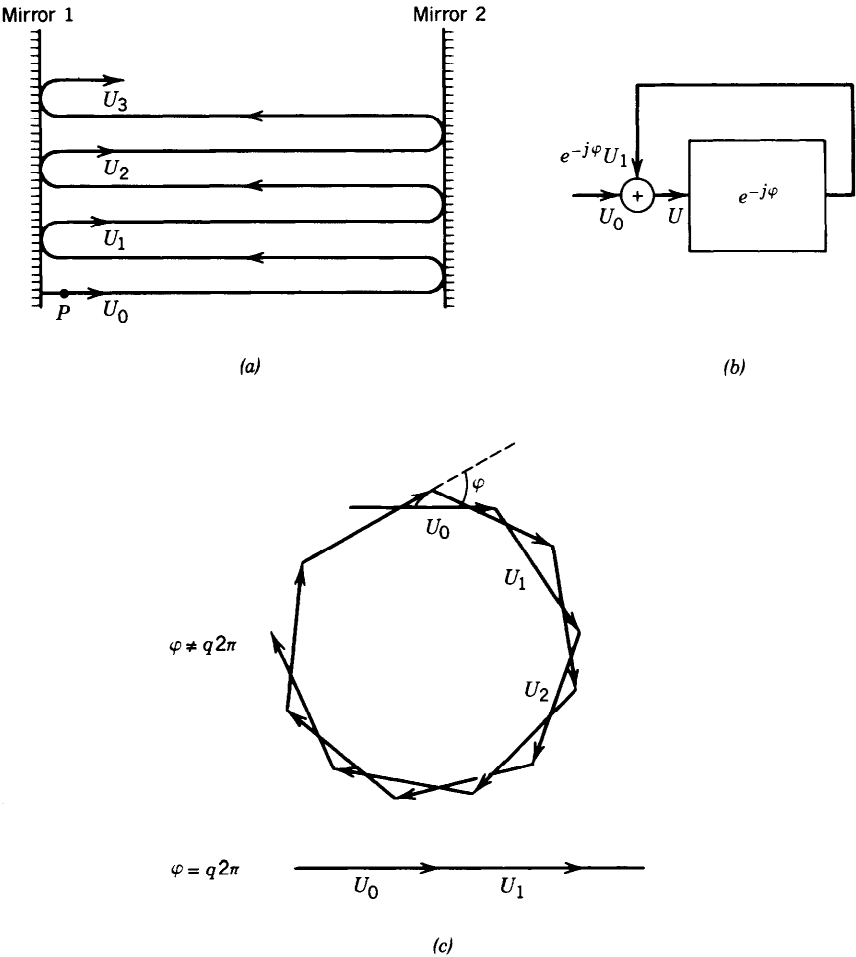


Figure 9.1-4 (a) A wave reflects back and forth between the resonator mirrors, suffering a phase shift φ each round trip. (b) Block diagram representing the optical feedback system. (c) Phasor diagram representing the sum $U = U_0 + U_1 + \dots$ for $\varphi \neq q2\pi$ and $\varphi = q2\pi$.

complex amplitude U_0 at point P traveling to the right along the axis of the resonator [see Fig. 9.1-4(a)]. The wave is reflected from mirror 2 and propagates back to mirror 1 where it is again reflected. Its amplitude at P then becomes U_1 . Yet another round trip results in a wave of complex amplitude U_2 , and so on *ad infinitum*. Because the original wave U_0 is monochromatic, it is “eternal.” Indeed, all of the partial waves U_0, U_1, U_2, \dots are monochromatic and perpetually coexist. Furthermore, their magnitudes are identical because there is no loss associated with the reflection and propagation. The total wave U is therefore represented by the sum of an infinite number of phasors of equal magnitude,

$$U = U_0 + U_1 + U_2 + \cdots, \quad (9.1-6)$$

as shown in Fig. 9.1-4(c).

The phase difference of two consecutive phasors imparted by a single round trip of propagation is $\varphi = k2d$. If the magnitude of the initial phasor is infinitesimal, the magnitude of each of these phasors must be infinitesimal. The magnitude of the sum of this infinite number of infinitesimal phasors is itself infinitesimal unless they are aligned, i.e., unless $\varphi = q2\pi$. Thus, an infinitesimal initial wave can result in the buildup of finite power in the resonator, but only if $\varphi = q2\pi$.

EXERCISE 9.1-1

Resonance Frequencies of a Ring Resonator. Derive an expression for the resonance frequencies of the three-mirror ring resonator shown in Fig. 9.1-5. Assume that each mirror reflection introduces a phase shift of π .

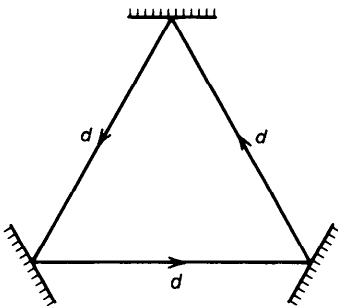


Figure 9.1-5 Three-mirror ring resonator.

Density of Modes

The number of modes per unit frequency is $1/\nu_F = 2d/c$ in each of the two orthogonal polarizations. Thus the density of modes $M(\nu)$, which is the number of modes per unit frequency per unit length of the resonator, is

$$M(\nu) = \frac{4}{c}. \quad (9.1-7)$$

Density of Modes
(One-Dimensional Resonator)

The number of modes in a resonator of length d within the frequency interval $\Delta\nu$ is therefore $(4/c)d\Delta\nu$. This represents the number of degrees of freedom for the optical waves existing in the resonator, i.e., the number of independent ways in which these waves may be arranged.

Losses and Resonance Spectral Width

The strict condition on the frequencies of optical waves that are permitted to exist inside a resonator is relaxed when the resonator has losses. Consider again Fig. 9.1-4(a) and follow a wave U_0 in its excursions between the two mirrors. The result is an infinite sum of phasors as in Fig. 9.1-4(c). As previously, the phase difference imparted by a single propagation round trip is

$$\varphi = 2kd = \frac{4\pi\nu d}{c}. \quad (9.1-8)$$

In the presence of loss, however, the phasors are not of equal magnitude. The magnitude ratio of two consecutive phasors is the round-trip amplitude attenuation factor ρ introduced by the two mirror reflections and by absorption in the medium. The intensity attenuation factor is therefore ρ^2 . Thus $U_1 = hU_0$, where $h = \rho e^{-j\varphi}$. The phasor U_2 is related to U_1 by this same complex factor h , as are all consecutive phasors. The net result is the superposition of an infinite number of waves, separated by equal phase shifts, but with amplitudes that are geometrically reduced. It is readily seen that $U = U_0 + U_1 + U_2 + \cdots = U_0 + hU_0 + h^2U_0 + \cdots = U_0(1 + h + h^2 + \cdots) = U_0/(1 - h)$. The relation $U = U_0/(1 - h)$ may be easily verified from the simple feedback configuration provided in Fig. 9.1-4(b). The intensity in the resonator

$$\begin{aligned} I = |U|^2 &= |U_0|^2 / |1 - \rho e^{-j\varphi}|^2 = I_0 / [(1 - \rho \cos \varphi)^2 + (\rho \sin \varphi)^2] \\ &= I_0 / (1 + \rho^2 - 2\rho \cos \varphi) = I_0 / [(1 - \rho)^2 + 4\rho \sin^2(\varphi/2)] \end{aligned}$$

is found to be

$$I = \frac{I_{\max}}{1 + (2\mathcal{F}/\pi)^2 \sin^2(\varphi/2)}, \quad I_{\max} = \frac{I_0}{(1 - \rho)^2}. \quad (9.1-9)$$

Here $I_0 = |U_0|^2$ is the intensity of the initial wave, and

$$\mathcal{F} = \frac{\pi\rho^{1/2}}{1 - \rho} \quad (9.1-10)$$

is a parameter known as the **finesse** of the resonator.

The intensity I is a periodic function of φ with period 2π . If \mathcal{F} is large, then I has sharp peaks centered about the values $\varphi = q2\pi$ (when all the phasors are aligned). The peaks have a full width at half maximum (FWHM) given by $\Delta\varphi = 2\pi/\mathcal{F}$. The width of each peak is \mathcal{F} times smaller than the period. The treatment given here is not unlike that provided in Sec. 2.5B on pages 70–72. One superficial difference (that has no bearing on the results) is the choice of $h = \rho e^{-j\varphi}$, which is used since successive phasors arise from the delay of the wave as it bounces between the mirrors.

The dependence of I on ν , which is the spectral response of the resonator, has a similar periodic behavior since $\varphi = 4\pi\nu d/c$ is proportional to ν . This resonance profile,

$$I = \frac{I_{\max}}{1 + (2\mathcal{F}/\pi)^2 \sin^2(\pi\nu/\nu_F)}, \quad (9.1-11)$$

Spectral Response of the
Fabry – Perot Resonator

is shown in Fig. 9.1-6, where $\nu_F = c/2d$. The maximum $I = I_{\max}$ is achieved at the resonance frequencies

$$\nu = \nu_q = q\nu_F, \quad q = 1, 2, \dots, \quad (9.1-12)$$

whereas the minimum value

$$I_{\min} = \frac{I_{\max}}{1 + (2\mathcal{F}/\pi)^2}, \quad (9.1-13)$$

occurs at the midpoints between the resonances. When the finesse is large ($\mathcal{F} \gg 1$), the resonator spectral response is sharply peaked about the resonance frequencies and I_{\min}/I_{\max} is small. In that case, the FWHM of the resonance peak is $\delta\nu = (c/4\pi d) \Delta\varphi = \nu_F/\mathcal{F}$, as was shown in Sec. 2.5B.

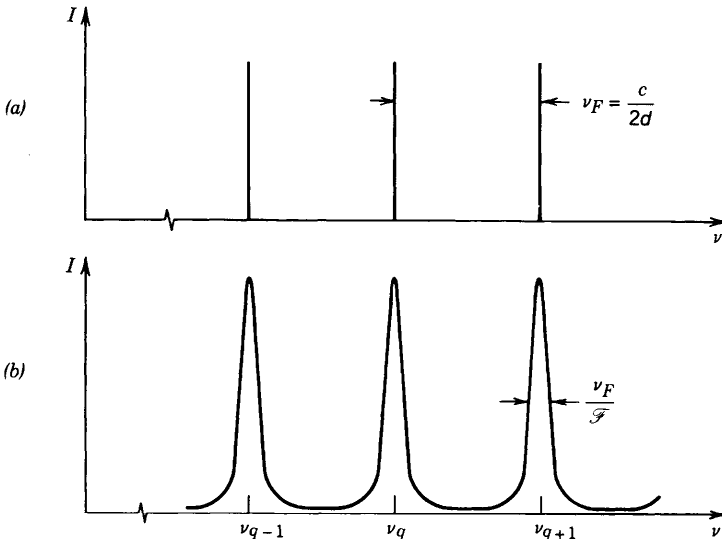


Figure 9.1-6 (a) A lossless resonator ($\mathcal{F} = \infty$) in the steady state can sustain light waves only at the precise resonance frequencies ν_q . (b) A lossy resonator sustains waves at all frequencies, but the attenuation resulting from destructive interference increases at frequencies away from the resonances.

In short, two parameters characterize the spectral response of the Fabry–Perot resonator:

- The spacing between adjacent resonance frequencies

$$\nu_F = \frac{c}{2d}; \quad (9.1-14)$$

Frequency Spacing of
Adjacent Resonator Modes

- The width of the resonances $\delta\nu$. When $\mathcal{F} \gg 1$,

$$\delta\nu \approx \frac{\nu_F}{\mathcal{F}}. \quad (9.1-15)$$

Spectral Width of
Resonator Modes

The resonance linewidth is inversely proportional to the finesse. Since the finesse decreases with increasing loss, the spectral width increases with increasing loss.

Sources of Resonator Loss

The two principal sources of loss in optical resonators are:

- Losses attributable to absorption and scattering in the medium between the mirrors. The round-trip power attenuation factor associated with these processes is $\exp(-2\alpha_s d)$, where α_s is the absorption coefficient of the medium.
- Losses arising from imperfect reflection at the mirrors. There are two underlying sources of reduced reflection: (1) A partially transmitting mirror is often used in a resonator to permit light to escape from it; and (2) the finite size of the mirrors causes a fraction of the light to leak around the mirrors and thereby to be lost. This also modifies the spatial distribution of the reflected wave by truncating it to the size of the mirror. The reflected light produces a diffraction pattern at the opposite mirror which is again truncated. Such diffraction loss may be regarded as an effective reduction of the mirror reflectance. Further details regarding diffraction loss are provided in Sec. 9.2E.

For mirrors of reflectances $\mathcal{R}_1 = r_1^2$ and $\mathcal{R}_2 = r_2^2$, the wave intensity decreases by the factor $\mathcal{R}_1 \mathcal{R}_2$ in the course of the two reflections associated with a single round trip. The overall intensity attenuation factor is therefore

$$r^2 = \mathcal{R}_1 \mathcal{R}_2 \exp(-2\alpha_s d), \quad (9.1-16)$$

which is usually written in the form

$$r^2 = \exp(-2\alpha_r d), \quad (9.1-17)$$

where α_r is an effective overall distributed-loss coefficient. Equations (9.1-16) and (9.1-17) provide

$$\alpha_r = \alpha_s + \frac{1}{2d} \ln \frac{1}{\mathcal{R}_1 \mathcal{R}_2}. \quad (9.1-18)$$

Loss Coefficient

This can also be written as

$$\alpha_r = \alpha_s + \alpha_{m1} + \alpha_{m2},$$

where the quantities

$$\alpha_{m1} = \frac{1}{2d} \ln \frac{1}{\mathcal{R}_1}, \quad \alpha_{m2} = \frac{1}{2d} \ln \frac{1}{\mathcal{R}_2}$$

represent the loss coefficients attributed to mirrors 1 and 2, respectively.

The loss coefficient can be cast in a simpler form for mirrors of high reflectance. If $\mathcal{R}_1 \approx 1$, then $\ln(1/\mathcal{R}_1) = -\ln(\mathcal{R}_1) = -\ln[1 - (1 - \mathcal{R}_1)] \approx 1 - \mathcal{R}_1$, where we have used the approximation $\ln(1 - \Delta) \approx -\Delta$, which is valid for $|\Delta| \ll 1$. This allows us to write

$$\alpha_{m1} \approx \frac{1 - \mathcal{R}_1}{2d}. \quad (9.1-19)$$

Similarly, if $\mathcal{R}_2 \approx 1$, we have $\alpha_{m2} \approx (1 - \mathcal{R}_2)/2d$. If, furthermore, $\mathcal{R}_1 = \mathcal{R}_2 = \mathcal{R} \approx 1$, then

$$\alpha_r \approx \alpha_s + \frac{1 - \mathcal{R}}{d}. \quad (9.1-20)$$

The finesse \mathcal{F} can be expressed as a function of the effective loss coefficient α_r by substituting (9.1-17) in (9.1-10), which provides

$$\mathcal{F} = \frac{\pi \exp(-\alpha_r d/2)}{1 - \exp(-\alpha_r d)}. \quad (9.1-21)$$

The finesse decreases with increasing loss, as shown in Fig. 9.1-7. If the loss factor

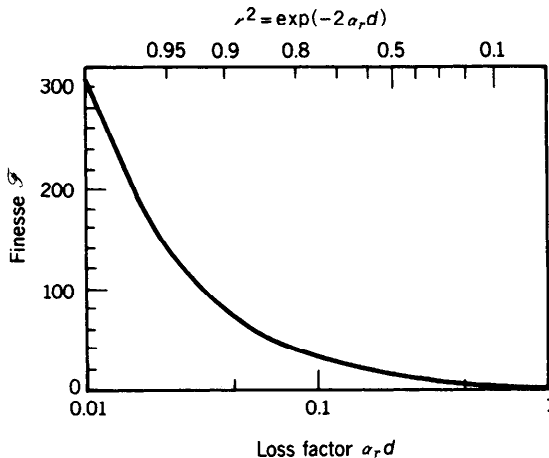


Figure 9.1-7 Finesse of an optical resonator versus the loss factor $\alpha_r d$. The round-trip attenuation factor $r^2 = \exp(-2\alpha_r d)$.

$\alpha_r d \ll 1$, then $\exp(-\alpha_r d) \approx 1 - \alpha_r d$, whereupon

$$\mathcal{F} \approx \frac{\pi}{\alpha_r d}.$$

(9.1-22)

Relation Between
Finesse and Loss Factor

This demonstrates that the finesse is inversely proportional to the loss factor $\alpha_r d$ in this limit.

EXERCISE 9.1-2

Resonator Modes and Spectral Width. Determine the frequency spacing, and spectral width, of the modes of a Fabry–Perot resonator whose mirrors have reflectances 0.98 and 0.99 and are separated by a distance $d = 100$ cm. The medium has refractive index $n = 1$ and negligible losses. Is the approximation used to derive (9.1-22) appropriate in this case?

Photon Lifetime

The relationship between the resonance linewidth and the resonator loss may be viewed as a manifestation of the time–frequency uncertainty relation. Substituting (9.1-14) and (9.1-22) in (9.1-15), we obtain

$$\delta\nu \approx \frac{c/2d}{\pi/\alpha_r d} = \frac{c\alpha_r}{2\pi}. \quad (9.1-23)$$

Because α_r is the loss per unit length, $c\alpha_r$ is the loss per unit time. Defining the characteristic decay time

$$\tau_p = \frac{1}{c\alpha_r} \quad (9.1-24)$$

as the **resonator lifetime** or **photon lifetime**, we obtain

$$\delta\nu = \frac{1}{2\pi\tau_p}. \quad (9.1-25)$$

The time–frequency uncertainty product is therefore $\delta\nu \cdot \tau_p = 1/2\pi$. The resonance line broadening is seen to be governed by the decay of optical energy arising from resonator losses. An electric field that decays as $\exp(-t/2\tau_p)$, which corresponds to an energy that decays as $\exp(-t/\tau_p)$, has a Fourier transform that is proportional to $1/(1 + j4\pi\nu\tau_p)$ with a FWHM spectral width $\delta\nu = 1/2\pi\tau_p$.

In summary, three parameters are convenient for characterizing the losses in an optical resonator of length d : the finesse \mathcal{F} , the loss coefficient α_r (cm^{-1}), and the photon lifetime $\tau_p = 1/c\alpha_r$ (seconds). In addition, the quality factor Q can also be used for this purpose, as outlined below.

*The Quality Factor Q

The quality factor Q is often used to characterize electrical resonance circuits and microwave resonators. This parameter is defined as

$$Q = \frac{2\pi (\text{stored energy})}{\text{energy loss per cycle}}.$$

Large Q factors are associated with low-loss resonators. A series RLC circuit has resonance frequency $\nu_0 \approx 1/2\pi(LC)^{1/2}$ and quality factor $Q = 2\pi\nu_0 L/R$, where R , C , and L are the resistance, capacitance, and inductance of the resonance circuit, respectively.

The Q factor of an optical resonator may be determined by observing that stored energy is lost at the rate $c\alpha_r$ (per unit time), which is equivalent to the rate $c\alpha_r/\nu_0$ (per cycle), so that $Q = 2\pi[1/(c\alpha_r/\nu_0)]$. Since $\delta\nu = c\alpha_r/2\pi$,

$$Q = \frac{\nu_0}{\delta\nu}. \quad (9.1-26)$$

The quality factor is related to the resonator lifetime (photon lifetime) $\tau_p = 1/c\alpha_r$ by

$$Q = 2\pi\nu_0\tau_p. \quad (9.1-27)$$

By using (9.1-15), we find that Q is related to the finesse of the resonator by

$$Q = \frac{\nu_0}{\nu_F} \mathcal{F}. \quad (9.1-28)$$

Since optical resonator frequencies ν_0 are typically much greater than the mode spacing ν_F , $Q \gg \mathcal{F}$. The quality factor of an optical resonator is typically far greater than that of a resonator at microwave frequencies.

B. The Resonator as a Spectrum Analyzer

What fraction of the intensity of an optical wave of frequency ν incident on a Fabry-Perot etalon is transmitted through it? We proceed to demonstrate that the transmittance is high if the frequency of the optical wave coincides with one of the resonance frequencies ($\nu = \nu_q$). The attenuation at other frequencies depends on the lossiness of the resonator. A low-loss resonator can therefore be used as a spectrum analyzer.

A plane wave of complex amplitude U_i and intensity I_i entering a resonator undergoes multiple reflections and transmissions, as illustrated in Fig. 9.1-8. Defining the complex amplitude and intensity of the transmitted wave as U_t and I_t , respectively, we proceed to obtain an expression for the intensity transmittance $\mathcal{T}(\nu) = I_t/I_i$, as a function of the frequency of the wave ν .

Let r_1 and r_2 be the amplitude reflectances of the inner surfaces of mirrors 1 and 2, and t_1 and t_2 the amplitude transmittances of the mirrors, respectively. In accordance with our previous analysis, the intensity I of the sum U of the internal waves U_0, U_1, \dots is related to the intensity I_0 of the initial wave U_0 by (9.1-9), with $r = r_1 r_2$. The transmitted intensity I_t is, however, related to the total internal intensity by $I_t = |t_2|^2 I$, while the initial intensity I_0 is related to the incident intensity by $I_0 = |t_1|^2 I_i$. Thus $I_t/I_i = |t|^2 (I/I_0)$, where $t = t_1 t_2$. Finally, using (9.1-9), we obtain an

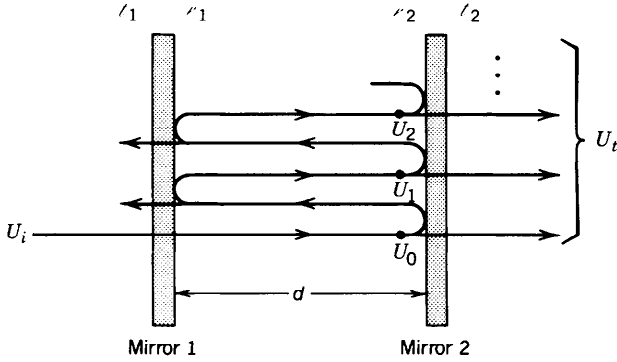


Figure 9.1-8 Transmission of a plane wave across a planar-mirror resonator (Fabry-Perot etalon).

expression for $\mathcal{T}(\nu) = I_t/I_i$:

$$\mathcal{T}(\nu) = \frac{\mathcal{T}_{\max}}{1 + (2\mathcal{F}/\pi)^2 \sin^2(\pi\nu/\nu_F)},$$

(9.1-29)

Transmittance of a
Fabry – Perot Resonator

where

$$\mathcal{T}_{\max} = \frac{|\ell|^2}{(1 - \rho)^2}, \quad \ell = \ell_1 \ell_2, \quad \rho = \rho_1 \rho_2, \quad (9.1-30)$$

and again

$$\mathcal{F} = \frac{\pi \rho^{1/2}}{1 - \rho}. \quad (9.1-31)$$

We conclude that the resonator transmittance $\mathcal{T}(\nu)$ has the same dependence on ν as that of the internal wave—sharply peaked functions surrounding the resonance frequencies. The width of each of these resonance peaks is a factor \mathcal{F} smaller than the spacing between them.

A Fabry-Perot etalon may therefore be used as a sharply tuned optical filter or spectrum analyzer. Because of the periodic nature of the spectral response, however, the spectral width of the measured light must be narrower than the frequency spacing $\nu_F = c/2d$ in order to avoid ambiguity. The quantity ν_F is therefore known as the **free spectral range**. The filter is tuned (i.e., the resonance frequencies are shifted) by adjusting the distance d between the mirrors. A slight change in mirror spacing Δd shifts the resonance frequency $\nu_q = qc/2d$ by a relatively large amount $\Delta\nu_q = -(qc/2d^2)\Delta d = -\nu_q \Delta d/d$. Although the frequency spacing ν_F also changes, it is by the far smaller amount $-\nu_F \Delta d/d$. Using an example with mirror separation $d = 1.5$ cm leads to a free spectral range $\nu_F = 10$ GHz when $n = 1$. For a typical optical frequency ($\nu = 10^{14}$ Hz), a change of d by a factor of 10^{-4} ($\Delta d = 1.5 \mu\text{m}$) translates the peak frequency by $\Delta\nu_q = 10$ GHz, whereas the free spectral range is altered by only 1 MHz becoming 9.999 GHz.

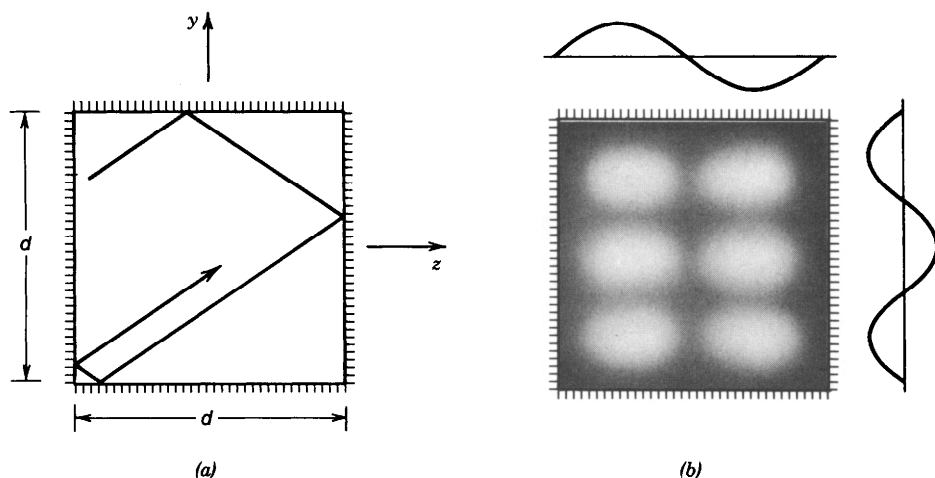


Figure 9.1-9 A two-dimensional planar-mirror resonator: (a) ray pattern; (b) standing-wave pattern with mode numbers $q_y = 3$ and $q_z = 2$.

C. Two- and Three-Dimensional Resonators[†]

Two-Dimensional Resonators

A two-dimensional planar-mirror resonator is constructed from two orthogonal pairs of parallel mirrors, e.g., a pair normal to the z axis and another pair normal to the y axis. Light is confined by a sequence of ray reflections in the z - y plane as illustrated in Fig. 9.1-9(a).

As for the one-dimensional Fabry–Perot resonator, the boundary conditions establish the resonator modes. If the mirror spacing is d , then the components of the wavevector $\mathbf{k} = (k_y, k_z)$ for standing waves are restricted to the values

$$k_y = \frac{q_y \pi}{d}, \quad k_z = \frac{q_z \pi}{d}, \quad q_y = 1, 2, \dots, \quad q_z = 1, 2, \dots, \quad (9.1-32)$$

where q_y and q_z are mode numbers in the y and z directions, respectively. This condition is a generalization of (9.1-2). Each pair of integers (q_y, q_z) represents a resonator mode $U(\mathbf{r}) \propto \sin(q_y \pi y/d) \sin(q_z \pi z/d)$, as illustrated in Fig. 9.1-9(b). The lowest-order mode is the (1, 1) mode since the modes $(q_y, 0)$ and $(0, q_z)$ have zero amplitude, viz., $U(\mathbf{r}) = 0$. Modes are conveniently represented by dots that mark their values of k_y and k_z on a periodic lattice of spacing π/d (Fig. 9.1-10).

The wavenumber k of a mode is the distance of the dot from the origin. Its frequency is $\nu = ck/2\pi$. The frequencies of the resonator modes are determined by using the relation

$$k^2 = k_y^2 + k_z^2 = \left(\frac{2\pi\nu}{c} \right)^2. \quad (9.1-33)$$

The number of modes in a given frequency band, $\nu_1 < \nu < \nu_2$, is determined by drawing two circles, of radii $k_1 = 2\pi\nu_1/c$ and $k_2 = 2\pi\nu_2/c$, and counting the number

[†]Although the material contained in this section is not used in the remainder of this chapter, it is required for Chap. 12 (Secs. 12.2B and 12.3B).

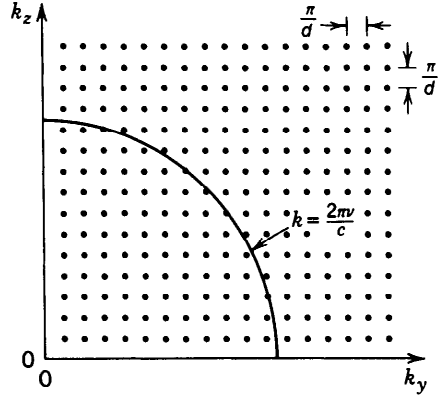


Figure 9.1-10 Dots denote the endpoints of the wavevectors $\mathbf{k} = (k_y, k_z)$ of modes in a two-dimensional resonator.

of dots that lie within that area. This procedure converts the allowed values of the vector \mathbf{k} into allowed values of the frequency ν .

EXERCISE 9.1-3

Density of Modes in a Two-Dimensional Resonator

- (a) Determine an approximate expression for the number of modes in a two-dimensional resonator with frequencies lying between 0 and ν , assuming that $2\pi\nu/c \gg \pi/d$, i.e., $d \gg \lambda/2$, and allowing for two orthogonal polarizations per mode number.
- (b) Show that the number of modes per unit area lying within the frequency interval between ν and $\nu + d\nu$ is $M(\nu)d\nu$, where the density of modes $M(\nu)$ (modes per unit area per unit frequency) at frequency ν is given by

$$M(\nu) = \frac{4\pi\nu}{c^2}.$$

(9.1-34)

Density of Modes

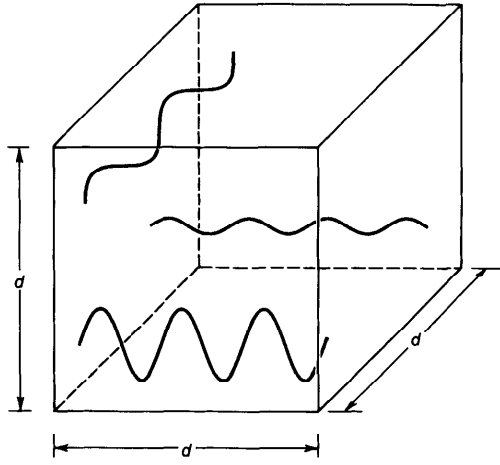
(Two-Dimensional Resonator)

Three-Dimensional Resonators

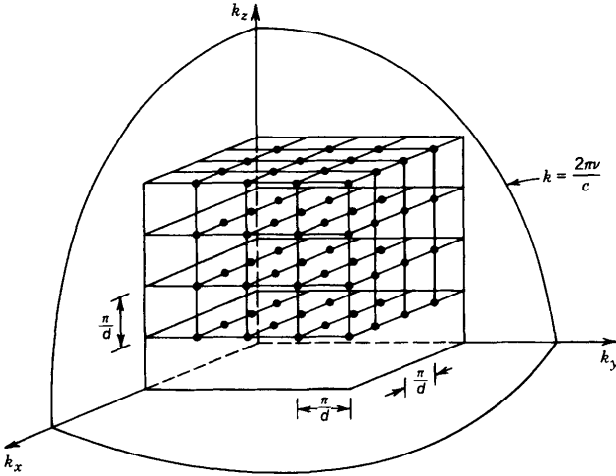
Consider now a resonator constructed of three pairs of parallel mirrors forming the walls of a closed box of size d . The structure is a three-dimensional resonator. Standing-wave solutions within the resonator require that components of the wavevector $\mathbf{k} = (k_x, k_y, k_z)$ are discretized to obey

$$k_x = \frac{q_x\pi}{d}, \quad k_y = \frac{q_y\pi}{d}, \quad k_z = \frac{q_z\pi}{d}, \quad q_x, q_y, q_z = 1, 2, \dots, \quad (9.1-35)$$

where q_x , q_y , and q_z are positive integers representing the respective mode numbers. Each mode, which is characterized by the three integers (q_x, q_y, q_z) , is represented by a



(a)



(b)

Figure 9.1-11 (a) Waves in a three-dimensional cubic resonator. (b) The endpoints of the wavevectors (k_x, k_y, k_z) of the modes in a three-dimensional resonator are marked by dots. The wavenumber k of a mode is the distance from the origin to the dot. All modes of frequency smaller than ν lie inside the positive octant of a sphere of radius $k = 2\pi\nu/c$.

dot in the (k_x, k_y, k_z) -space in Fig. 9.1-11. The values of the wavenumbers k and the corresponding resonance frequencies ν satisfy

$$k^2 = k_x^2 + k_y^2 + k_z^2 = \left(\frac{2\pi\nu}{c} \right)^2. \quad (9.1-36)$$

The surface of constant frequency ν is a sphere of radius $k = 2\pi\nu/c$.

Density of Modes

The number of modes lying in the frequency interval between 0 and ν corresponds to the number of points lying in the volume of the positive octant of a sphere of radius k in the k diagram [Fig. 9.1-11(b)]. Because it is analytically difficult to enumerate these modes, we resort to a continuous approximation, the validity of which depends on the relative values of the bandwidth of interest and the frequency interval between successive modes. The number of modes in the positive octant of a sphere of radius k is $2(\frac{1}{8})(4\pi k^3/3)/(\pi/d)^3 = (k^3/3\pi^2)d^3$. The initial factor of 2 accounts for the two possible polarizations of each mode, whereas the denominator $(\pi/d)^3$ represents the volume in k space per point. Since $k = 2\pi\nu/c$, the number of modes lying between 0 and ν is $[(2\pi\nu/c)^3/3\pi^2]d^3 = (8\pi\nu^3/3c^3)d^3$. The number of modes in the incremental frequency interval lying between ν and $\nu + \Delta\nu$ is therefore given by $(d/d\nu)[(8\pi\nu^3/3c^3)d^3]\Delta\nu = (8\pi\nu^2/c^3)d^3\Delta\nu$. The density of modes $M(\nu)$, i.e., the number of modes per unit volume of the resonator per unit bandwidth surrounding the frequency ν , is therefore

$$M(\nu) = \frac{8\pi\nu^2}{c^3}.$$

(9.1-37)

Density of Modes
(Three-Dimensional Resonator)

The number of modes per unit volume within an arbitrary frequency interval $\nu_1 < \nu < \nu_2$ is the integral $\int_{\nu_1}^{\nu_2} M(\nu) d\nu$.

The density of modes $M(\nu)$ is a quadratically increasing function of frequency so that the number of modes within a fixed bandwidth $\Delta\nu$ increases with frequency ν in the manner indicated in Fig. 9.1-12. At $\nu = 3 \times 10^{14}$ ($\lambda_o = 1 \text{ }\mu\text{m}$), $M(\nu) = 0.08$ modes/cm³-Hz. Within a band of width 1 GHz, for example, there are $\approx 8 \times 10^7$ modes/cm³.

The density of modes in two and three dimensions were derived on the basis of square and cubic geometry, respectively. Nevertheless, the results are applicable for arbitrary geometries, provided that the resonator dimensions are large in comparison with the wavelength.

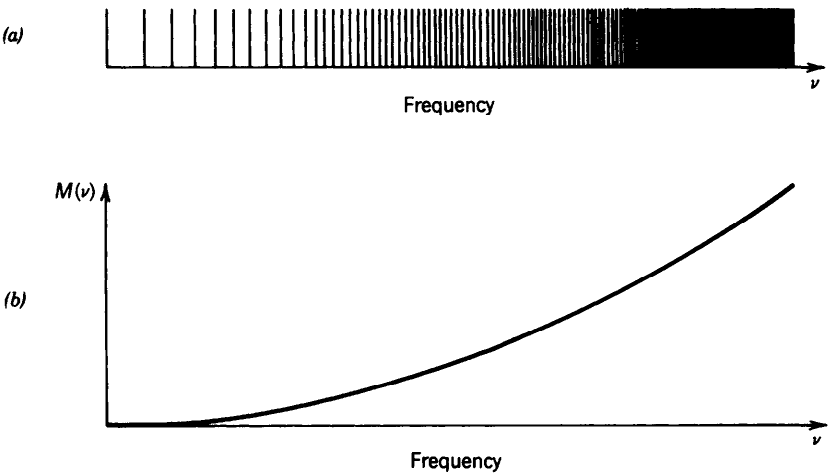


Figure 9.1-12 (a) The frequency spacing between adjacent modes decreases as the frequency increases. (b) The density of modes $M(\nu)$ for a three-dimensional optical resonator is a quadratically increasing function of frequency.

Finally, we point out that the enumeration of the electromagnetic modes presented here is mathematically identical to the calculation of the allowed quantum states of electrons confined within perfectly reflecting walls. The latter model is of importance in determining the density of allowed electron states as a function of energy in a semiconductor material (see Sec. 15.1C).

9.2 SPHERICAL-MIRROR RESONATORS

The planar-mirror resonator configuration discussed in the preceding section is highly sensitive to misalignment. If the mirrors are not perfectly parallel, or the rays are not perfectly normal to the mirror surfaces, they undergo a sequence of lateral displacements that eventually causes them to wander out of the resonator. Spherical-mirror resonators, in contrast, provide a more stable configuration for the confinement of light that renders them less sensitive to misalignment under certain geometrical conditions.

A spherical-mirror resonator is constructed of two spherical mirrors of radii R_1 and R_2 separated by a distance d (Fig. 9.2-1). The centers of the mirrors define the optical axis (z axis), about which the system exhibits circular symmetry. Each of the mirrors can be concave ($R < 0$) or convex ($R > 0$). The planar-mirror resonator is a special case for which $R_1 = R_2 = \infty$. We first examine the conditions for the confinement of optical rays. Then we determine the resonator modes. Finally, the effect of finite mirror size is discussed briefly.

A. Ray Confinement

Our initial approach is to use ray optics to determine the conditions of confinement for light rays in a spherical-mirror resonator. We consider only meridional rays (rays lying in a plane that passes through the optical axis) and limit ourselves to paraxial rays (rays that make small angles with the optical axis). The matrix-optics methods introduced in Sec. 1.4, which are valid only for paraxial rays, are used to study the trajectories of rays as they travel inside the resonator.

A resonator is a periodic optical system, since a ray travels through the same system after a round trip of two reflections. We may therefore make use of the analysis of periodic optical systems presented in Sec. 1.4D. Let y_m and θ_m be the position and inclination of an optical ray after m round trips, as illustrated in Fig. 9.2-2. Given y_m and θ_m , y_{m+1} and θ_{m+1} can be determined by tracing the ray through the system.

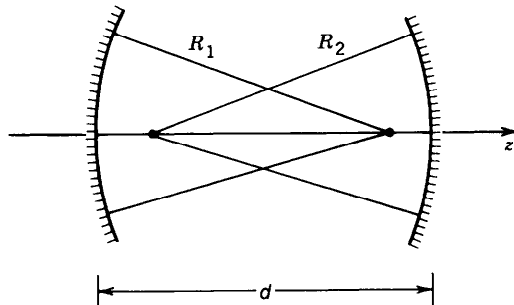


Figure 9.2-1 Geometry of a spherical-mirror resonator. In this case both mirrors are concave (their radii of curvature are negative).

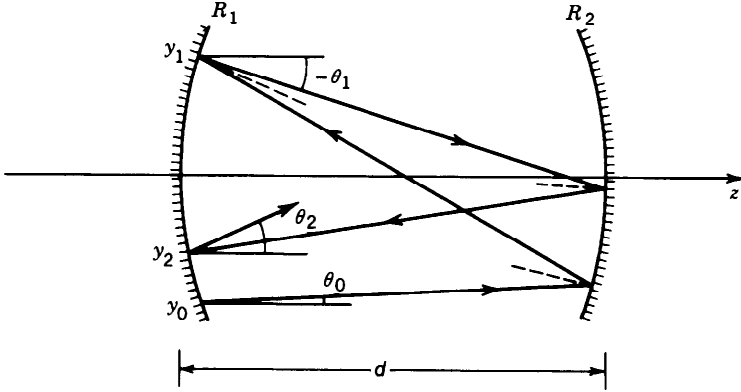


Figure 9.2-2 The position and inclination of a ray after m round trips are represented by y_m and θ_m , respectively, where $m = 0, 1, 2, \dots$. In this diagram, $\theta_1 < 0$ since the ray is going downward.

For paraxial rays, where all angles are small, the relation between (y_{m+1}, θ_{m+1}) and (y_m, θ_m) is linear and can be written in the matrix form

$$\begin{bmatrix} y_{m+1} \\ \theta_{m+1} \end{bmatrix} = \begin{bmatrix} A & B \\ C & D \end{bmatrix} \begin{bmatrix} y_m \\ \theta_m \end{bmatrix}. \quad (9.2-1)$$

The round-trip ray-transfer matrix for Fig. 9.2-2:

$$\begin{bmatrix} A & B \\ C & D \end{bmatrix} = \begin{bmatrix} 1 & 0 \\ \frac{2}{R_1} & 1 \end{bmatrix} \begin{bmatrix} 1 & d \\ 0 & 1 \end{bmatrix} \begin{bmatrix} 1 & 0 \\ \frac{2}{R_2} & 1 \end{bmatrix} \begin{bmatrix} 1 & d \\ 0 & 1 \end{bmatrix}$$

is a product of ray-transfer matrices representing, from right to left [see (1.4-3) and (1.4-8)]:

- propagation a distance d through free space,
- reflection from a mirror of radius R_2 ,
- propagation a distance d through free space,
- reflection from a mirror of radius R_1 .

As shown in Sec. 1.4D, the solution of the difference equation (9.2-1) is $y_m = y_{\max} F^m \sin(m\varphi + \varphi_0)$, where $F^2 = AD - BC$, $\varphi = \cos^{-1}(b/F)$, $b = (A + D)/2$, and y_{\max} and φ_0 are constants to be determined from the initial position and inclination of the ray. For the case at hand $F = 1$, so that

$$y_m = y_{\max} \sin(m\varphi + \varphi_0), \quad (9.2-2)$$

$$\varphi = \cos^{-1} b, \quad b = 2 \left(1 + \frac{d}{R_1} \right) \left(1 + \frac{d}{R_2} \right) - 1.$$

The solution (9.2-2) is harmonic (and therefore bounded) provided that $\varphi = \cos^{-1}b$ is real. This is ensured if $|b| \leq 1$, i.e., if $-1 \leq b \leq 1$ or $0 \leq (1 + d/R_1)(1 + d/R_2) \leq 1$. It is convenient to write this condition in terms of the parameters $g_1 = 1 + d/R_1$ and

$g_2 = 1 + d/R_2$, which are known as the **g parameters**,

$$0 \leq g_1 g_2 \leq 1.$$

(9.2-3)

Confinement Condition

When this condition is not satisfied, φ is imaginary so that y_m in (9.2-2) becomes a hyperbolic sine function of m which increases without bound. The resonator is then said to be **unstable**. At the boundary of the confinement condition (when the inequalities are equalities), the resonator is said to be **conditionally stable**; slight errors in alignment render it unstable.

A useful graphical representation of the confinement condition (Fig. 9.2-3) identifies each combination (g_1, g_2) of the two g parameters of a resonator as a point in a g_2 versus g_1 diagram. The left inequality in (9.2-3) is equivalent to $\{g_1 \geq 0 \text{ and } g_2 \geq 0\}$; or $g_1 \leq 0 \text{ and } g_2 \leq 0\}$; i.e., all stable points (g_1, g_2) must lie in the first or third quadrant. The right inequality in (9.2-3) signifies that stable points (g_1, g_2) must lie in a region bounded by the hyperbola $g_1 g_2 = 1$. The unshaded area in Fig. 9.2-3 represents the region for which both inequalities are satisfied, indicating that the resonator is stable.

Symmetrical resonators, by definition, have identical mirrors ($R_1 = R_2 = R$) so that $g_1 = g_2 = g$. The condition of stability is then $g^2 \leq 1$, or $-1 \leq g \leq 1$, so that

$$0 \leq \frac{d}{(-R)} \leq 2.$$

(9.2-4)

Confinement Condition
(Symmetrical Resonator)

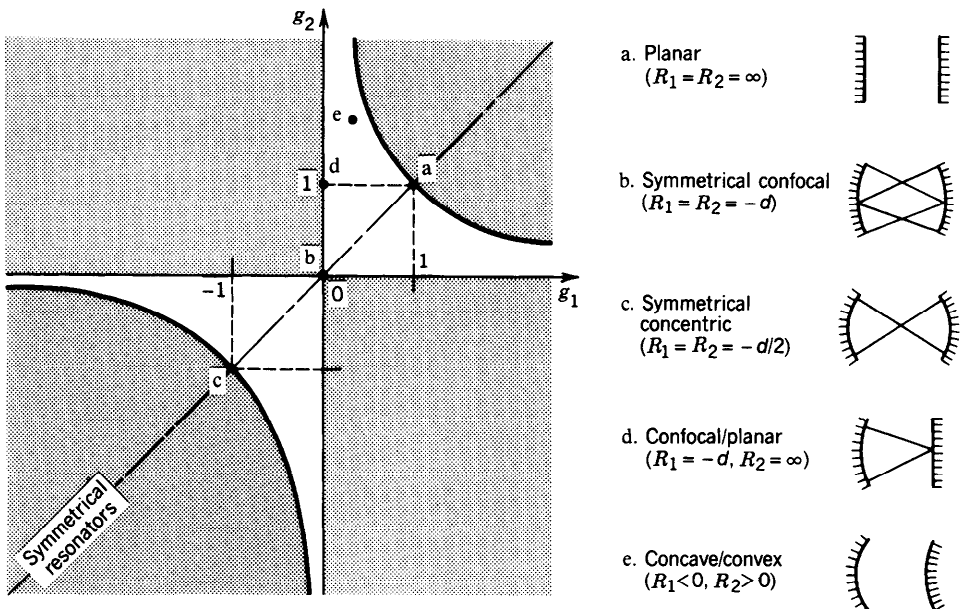


Figure 9.2-3 Resonator stability diagram. A spherical-mirror resonator is stable if the parameters $g_1 = 1 + d/R_1$ and $g_2 = 1 + d/R_2$ lie in the unshaded regions bounded by the lines $g_1 = 0$ and $g_2 = 0$, and the hyperbola $g_2 = 1/g_1$. R is negative for a concave mirror and positive for a convex mirror. Various special configurations are indicated by letters. All symmetrical resonators lie along the line $g_2 = g_1$.

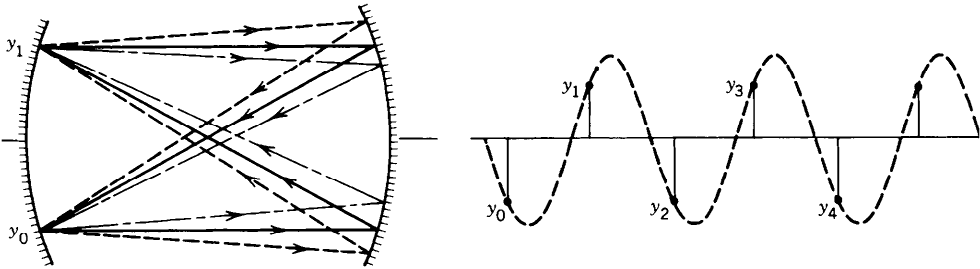


Figure 9.2-4 All paraxial rays in a symmetrical confocal resonator retrace themselves after two round trips, regardless of their original position and inclination. Angles are exaggerated in this drawing for the purpose of illustration.

These resonators are represented in Fig. 9.2-3 by points along the line $g_2 = g_1$. To satisfy (9.2-4) a stable symmetrical resonator must use concave mirrors ($R < 0$) whose radii are greater than half the resonator length. Three points within this interval are of special interest: $d/(-R) = 0, 1$, and 2 , corresponding to **planar**, **confocal**, and **concentric resonators**, respectively.

In the symmetrical confocal resonator, $(-R) = d$, so that the center of curvature of each mirror lies on the other. Thus in (9.2-2), $b = -1$, $\varphi = \pi$, and the ray position is $y_m = y_{\max} \sin(m\pi + \varphi_0)$, i.e., $y_m = (-1)^m y_0$. Rays initiated at position y_0 , at any inclination, are imaged to position $y_1 = -y_0$, then imaged again to position $y_2 = y_0$, and so on, repeatedly. Each ray retraces itself after two round trips (Fig. 9.2-4). All paraxial rays are therefore confined, no matter what their original position and inclination. This is to be compared with the planar-mirror resonator, for which only rays of zero inclination retrace themselves.

In summary, the confinement condition for paraxial rays in a spherical-mirror resonator, constructed of mirrors of radii R_1 and R_2 separated by a distance d , is $0 \leq g_1 g_2 \leq 1$, where $g_1 = 1 + d/R_1$ and $g_2 = 1 + d/R_2$.

EXERCISE 9.2-1

Maximum Resonator Length for Confined Rays. A resonator is constructed using concave mirrors of radii 50 cm and 100 cm. Determine the maximum resonator length for which rays satisfy the confinement condition.

B. Gaussian Modes

Although the ray-optics approach considered in the preceding section is useful for determining the geometrical conditions under which rays are confined, it cannot provide information about the spatial intensity distributions and resonance frequencies of the resonator modes. We now proceed to show that Gaussian beams are modes of

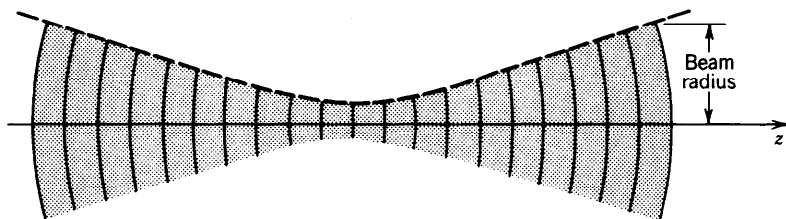


Figure 9.2-5 Gaussian beam wavefronts (solid curves) and beam radius (dashed curve).

the spherical-mirror resonator; Gaussian beams provide solutions of the Helmholtz equation under the boundary conditions imposed by the spherical-mirror resonator.

Gaussian Beams

As discussed in Chap. 3, a Gaussian beam is a circularly symmetric wave whose energy is confined about its axis (the z axis) and whose wavefront normals are paraxial rays (Fig. 9.2-5). In accordance with (3.1-12), at an axial distance z from the beam waist the beam intensity I varies in the transverse x - y plane as the Gaussian distribution $I = I_0[W_0/W(z)]^2 \exp[-2(x^2 + y^2)/W^2(z)]$. Its width is given by (3.1-8):

$$W(z) = W_0 \left[1 + \left(\frac{z}{z_0} \right)^2 \right]^{1/2}, \quad (9.2-5)$$

where z_0 is the distance, known as the Rayleigh range, at which the beam wavefronts are most curved. The beam width (radius) $W(z)$ increases in both directions from its minimum value W_0 at the beam waist ($z = 0$). The radius of curvature of the wavefronts, which is given by (3.1-9),

$$R(z) = z + \frac{z_0^2}{z} \quad (9.2-6)$$

decreases from ∞ at $z = 0$, to a minimum value at $z = z_0$, and thereafter grows linearly with z for large z . For $z > 0$, the wave diverges and $R(z) > 0$; for $z < 0$, the wave converges and $R(z) < 0$. The Rayleigh range z_0 is related to the beam waist radius W_0 by (3.1-11):

$$z_0 = \frac{\pi W_0^2}{\lambda}. \quad (9.2-7)$$

The Gaussian Beam Is a Mode of the Spherical-Mirror Resonator

A Gaussian beam reflected from a spherical mirror will retrace the incident beam if the radius of curvature of its wavefront is the same as the mirror radius (see Sec. 3.2C). Thus, if the radii of curvature of the wavefronts of a Gaussian beam at planes separated by a distance d match the radii of two mirrors separated by the same distance d , a beam incident on the first mirror will reflect and retrace itself to the second mirror, where it once again will reflect and retrace itself back to the first mirror, and so on. The beam can then exist self-consistently within the spherical-mirror resonator, satisfying the Helmholtz equation and the boundary conditions imposed by the mirrors. The Gaussian beam is then said to be a mode of the spherical-mirror resonator (provided that the phase also retraces itself, as discussed in Sec. 9.2C).

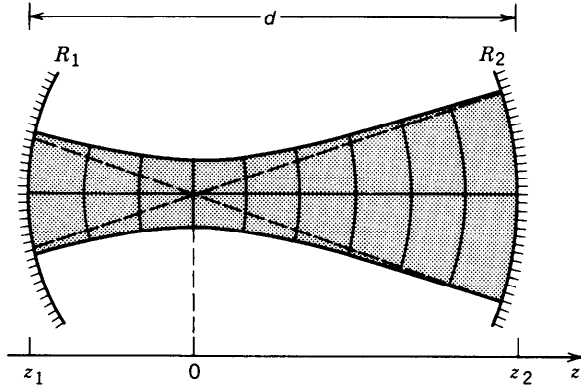


Figure 9.2-6 Fitting a Gaussian beam to two mirrors of radii R_1 and R_2 separated by a distance d . In this diagram both mirrors are concave (R_1 , R_2 , and z_1 are negative).

We now proceed to determine the Gaussian beam that matches a spherical-mirror resonator with mirrors of radii R_1 and R_2 separated by the distance d . This is illustrated in Fig. 9.2-6 for the special case when both mirrors are concave ($R_1 < 0$ and $R_2 < 0$).

The z axis is defined by the centers of the mirrors. The center of the beam, which is yet to be determined, is assumed to be located at the origin $z = 0$; mirrors R_1 and R_2 are located at positions z_1 and

$$z_2 = z_1 + d, \quad (9.2-8)$$

respectively. (A negative value for z_1 indicates that the center of the beam lies to the right of mirror 1; a positive value indicates that it lies to the left.) The values of z_1 and z_2 are determined by matching the radius of curvature of the beam, $R(z) = z + z_0^2/z$, to the radii R_1 at z_1 and R_2 at z_2 . Careful attention must be paid to the signs. If both mirrors are concave, they have negative radii. But the beam radius of curvature was defined to be positive for $z > 0$ (at mirror 2) and negative for $z < 0$ (at mirror 1). We therefore equate $R_1 = R(z_1)$ but $-R_2 = R(z_2)$, i.e.,

$$R_1 = z_1 + \frac{z_0^2}{z_1} \quad (9.2-9)$$

$$-R_2 = z_2 + \frac{z_0^2}{z_2}. \quad (9.2-10)$$

Solving (9.2-8), (9.2-9), and (9.2-10) for z_1 , z_2 , and z_0 leads to

$$z_1 = \frac{-d(R_2 + d)}{R_2 + R_1 + 2d}, \quad z_2 = z_1 + d \quad (9.2-11)$$

$$z_0^2 = \frac{-d(R_1 + d)(R_2 + d)(R_2 + R_1 + d)}{(R_2 + R_1 + 2d)^2}. \quad (9.2-12)$$

Having determined the location of the beam center and the depth of focus $2z_0$, everything about the beam is known (see Sec. 3.1B). The waist radius is $W_0 =$

$(\lambda z_0/\pi)^{1/2}$, and the beam radii at the mirrors are

$$W_i = W_0 \left[1 + \left(\frac{z_i}{z_0} \right)^2 \right]^{1/2}, \quad i = 1, 2. \quad (9.2-13)$$

A similar problem has been addressed in Chap. 3 (Exercise 3.1-5).

In order that the solution (9.2-11)–(9.2-12) indeed represent a Gaussian beam, z_0 must be real. An imaginary value of z_0 signifies that the Gaussian beam is in fact a paraboloidal wave, which is an unconfined solution (see Sec. 3.1A). Using (9.2-12), it is not difficult to show that the condition $z_0^2 > 0$ is equivalent to

$$0 \leq \left(1 + \frac{d}{R_1} \right) \left(1 + \frac{d}{R_2} \right) \leq 1, \quad (9.2-14)$$

which is precisely the confinement condition required by ray optics, as set forth in (9.2-3).

EXERCISE 9.2-2

A Plano-Concave Resonator. When mirror 1 is planar ($R_1 = \infty$), determine the confinement condition, the depth of focus, and the beam radius at the waist and at each of the mirrors, as a function of $d/|R_2|$.

Gaussian Mode of a Symmetrical Spherical-Mirror Resonator

The results obtained in (9.2-11)–(9.2-13) simplify considerably for symmetrical resonators with concave mirrors. Substituting $R_1 = R_2 = -|R|$ into (9.2-11) provides $z_1 = -d/2$, $z_2 = d/2$. Thus the beam center lies at the center of the resonator, and

$$z_0 = \frac{d}{2} \left(2 \frac{|R|}{d} - 1 \right)^{1/2} \quad (9.2-15)$$

$$W_0^2 = \frac{\lambda d}{2\pi} \left(2 \frac{|R|}{d} - 1 \right)^{1/2} \quad (9.2-16)$$

$$W_1^2 = W_2^2 = \frac{\lambda d/\pi}{\{(d/|R|)[2 - (d/|R|)]\}^{1/2}}. \quad (9.2-17)$$

The confinement condition (9.2-14) becomes

$$0 \leq \frac{d}{|R|} \leq 2. \quad (9.2-18)$$

Given a resonator of fixed mirror separation d , we now examine the effect of increasing mirror curvature (increasing $d/|R|$) on the beam radius at the waist W_0 , and at the mirrors $W_1 = W_2$. The results are illustrated in Fig. 9.2-7. For a planar-mirror resonator, $d/|R| = 0$, so that W_0 and W_1 are infinite, corresponding to a plane wave

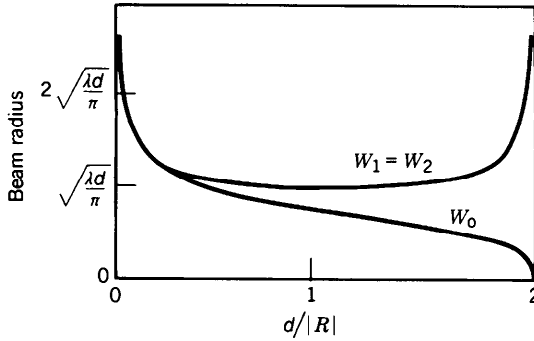


Figure 9.2-7 The beam radius at the waist, W_0 , and at the mirrors, $W_1 = W_2$, for a symmetrical spherical-mirror resonator with concave mirrors as a function of the ratio $d/|R|$. Symmetrical confocal and concentric resonators correspond to $d/|R| = 1$ and $d/|R| = 2$, respectively.

rather than a Gaussian beam. As $d/|R|$ increases, W_0 decreases until it vanishes for the concentric resonator ($d/|R| = 2$); at this point $W_1 = W_2 = \infty$. This is not surprising inasmuch as a spherical wave fits within a symmetrical concentric resonator (see Fig. 9.2-3).

The radius of the beam at the mirrors has its minimum value, $W_1 = W_2 = (\lambda d/\pi)^{1/2}$, when $d/|R| = 1$, i.e., for the symmetrical confocal resonator. In this case

$$z_0 = \frac{d}{2} \quad (9.2-19)$$

$$W_0 = \left(\frac{\lambda d}{2\pi} \right)^{1/2} \quad (9.2-20)$$

$$W_1 = W_2 = \sqrt{2} W_0. \quad (9.2-21)$$

The depth of focus $2z_0$ is then equal to the length of the resonator d , as shown in Fig. 9.2-8. This explains why the parameter $2z_0$ is sometimes called the confocal parameter. A long resonator has a long depth of focus. The waist radius is proportional to the square root of the mirror spacing. A Gaussian beam at $\lambda_0 = 633 \text{ nm}$ (one of the wavelengths of the helium–neon laser) in a resonator with $d = 100 \text{ cm}$, for example,

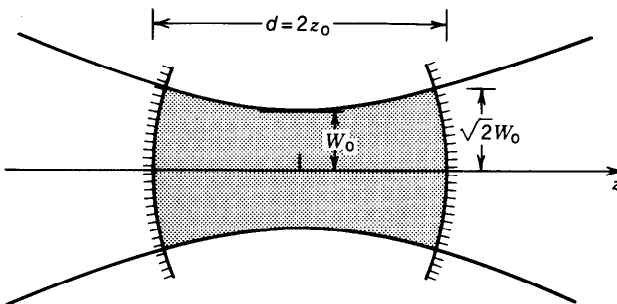


Figure 9.2-8 Gaussian beam in a symmetrical confocal resonator with concave mirrors. The depth of focus $2z_0$ equals the length of the resonator d . The beam radius at the mirrors is a factor of $\sqrt{2}$ greater than that at the waist.

has a waist radius $W_0 = (\lambda d/2\pi)^{1/2} = 0.32$ mm, whereas a 25-cm-long resonator supports a Gaussian beam of waist radius 0.16 mm at the same wavelength. The radius of the beam at each of the mirrors is greater than at the waist by a factor of $\sqrt{2}$.

C. Resonance Frequencies

As indicated in Sec. 9.2B, a Gaussian beam is a mode of the spherical-mirror resonator provided that the wavefront normals reflect onto themselves, always retracing the same path, and that the phase retraces itself as well.

The phase of a Gaussian beam, in accordance with (3.1-22), is

$$\varphi(\rho, z) = kz - \zeta(z) + \frac{k\rho^2}{2R(z)}$$

where $\zeta(z) = \tan^{-1}(z/z_0)$ and $\rho^2 = x^2 + y^2$. At points on the optical axis ($\rho = 0$), $\varphi(0, z) = kz - \zeta(z)$, so that the phase retardation relative to a plane wave is $\zeta(z)$. At the locations of the mirrors z_1 and z_2 ,

$$\varphi(0, z_1) = kz_1 - \zeta(z_1)$$

$$\varphi(0, z_2) = kz_2 - \zeta(z_2).$$

Because the mirror surface coincides with the wavefronts, all points on each mirror share the same phase. As the beam propagates from mirror 1 to mirror 2 its phase changes by

$$\begin{aligned} \varphi(0, z_2) - \varphi(0, z_1) &= k(z_2 - z_1) - [\zeta(z_2) - \zeta(z_1)] \\ &= kd - \Delta\zeta, \end{aligned} \tag{9.2-22}$$

where

$$\Delta\zeta = \zeta(z_2) - \zeta(z_1). \tag{9.2-23}$$

As the traveling wave completes a round trip between the two mirrors, therefore, its phase changes by $2kd - 2\Delta\zeta$.

In order that the beam truly retrace itself, the round-trip phase change must be a multiple of 2π , i.e., $2kd - 2\Delta\zeta = 2\pi q$, $q = 0, \pm 1, \pm 2, \dots$. Substituting $k = 2\pi\nu/c$ and $\nu_F = c/2d$, the frequencies ν_q that satisfy this condition are

$$\boxed{\nu_q = q\nu_F + \frac{\Delta\zeta}{\pi}\nu_F.} \tag{9.2-24}$$

Spherical-Mirror Resonator
Resonance Frequencies
(Gaussian Modes)

The frequency spacing of adjacent modes is $\nu_F = c/2d$, which is the same result as that obtained in Sec. 9.1A for the planar-mirror resonator. For spherical-mirror resonators, this frequency spacing is independent of the curvatures of the mirrors. The second term in (9.2-24), which does depend on the mirror curvatures, simply represents a displacement of all resonance frequencies.

EXERCISE 9.2-3

Resonance Frequencies of a Confocal Resonator. A symmetrical confocal resonator has a length $d = 30$ cm, and the medium has refractive index $n = 1$. Determine the frequency spacing ν_F and the displacement frequency $(\Delta\zeta/\pi)\nu_F$. Determine all the resonance frequencies that lie within the band $5 \times 10^{14} \pm 2 \times 10^9$ Hz.

D. Hermite – Gaussian Modes

In Sec. 3.3 it was shown that the Gaussian beam is not the only beam-like solution of the paraxial Helmholtz equation. An entire family of solutions, the Hermite–Gaussian family, exists. Although a Hermite–Gaussian beam of order (l, m) has the same wavefronts as a Gaussian beam, its amplitude distribution differs. The design of a resonator that “matches” a given beam (or the design of a beam that “fits” a given resonator) is therefore the same as in the Gaussian-beam case, regardless of (l, m) . It follows that the entire family of Hermite–Gaussian beams represents modes of the spherical-mirror resonator.

The resonance frequencies of the (l, m) mode do, however, depend on the indices (l, m) . This is because of the dependence of the axial phase delay on l and m . Using (3.3-9), the phase of the (l, m) mode on the beam axis is

$$\varphi(0, z) = kz - (l + m + 1)\zeta(z). \quad (9.2-25)$$

The phase shift encountered by a traveling wave undergoing a single round trip through a resonator of length d should be set equal to a multiple of 2π in order that the beam retrace itself. Thus

$$2kd - 2(l + m + 1)\Delta\zeta = 2\pi q, \quad q = 0, \pm 1, \pm 2, \dots, \quad (9.2-26)$$

where, as before, $\Delta\zeta = [\zeta(z_2) - \zeta(z_1)]$ and z_1, z_2 are the positions of the two mirrors. With $\nu_F = c/2d$, this yields the resonance frequencies

$$\nu_{l,m,q} = q\nu_F + (l + m + 1)\frac{\Delta\zeta}{\pi}\nu_F. \quad (9.2-27)$$

Spherical-Mirror
Resonator
Resonance Frequencies
(Hermite – Gaussian Modes)

Modes of different q , but the same (l, m) , have identical intensity distributions [see (3.3-11)]. They are known as **longitudinal** or **axial modes**. The indices (l, m) label different spatial dependences on the transverse coordinates x, y ; these represent different **transverse modes**, as illustrated in Fig. 3.3-2.

Equation (9.2-27) indicates that the resonance frequencies of the Hermite–Gaussian modes satisfy the following properties:

- Longitudinal modes corresponding to a given transverse mode (l, m) have resonance frequencies spaced by $\nu_F = c/2d$, i.e., $\nu_{l,m,q+1} - \nu_{l,m,q} = \nu_F$.
- All transverse modes, for which the sum of the indices $l + m$ is the same, have the same resonance frequencies.

- Two transverse modes (l, m) , (l', m') corresponding to the same longitudinal mode q have resonance frequencies spaced by

$$\nu_{l,m,q} - \nu_{l',m',q} = [(l + m) - (l' + m')] \frac{\Delta\zeta}{\pi} \nu_F. \quad (9.2-28)$$

This expression determines the frequency shift between the sets of longitudinal modes of indices (l, m) and (l', m') .

EXERCISE 9.2-4

Resonance Frequencies of the Symmetrical Confocal Resonator. Show that for a symmetrical confocal resonator the longitudinal modes associated with two transverse modes are either the same or are displaced by $\nu_F/2$, as illustrated in Fig. 9.2-9.

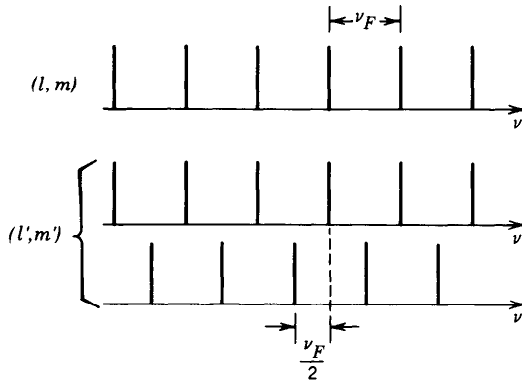


Figure 9.2-9 In a symmetrical confocal resonator, the longitudinal modes associated with two transverse modes of indices (l, m) and (l', m') are either aligned or displaced by half a longitudinal mode spacing.

*E. Finite Apertures and Diffraction Loss

Since Gaussian and Hermite–Gaussian beams have infinite transverse extent and since the resonator mirrors are of finite extent, a portion of the optical power escapes from the resonator on each pass. An estimate of the power loss may be determined by calculating the fractional power of the beam that is not intercepted by the mirror. If the beam is Gaussian with radius W and the mirror is circular with radius $a = 2W$, for example, a small fraction, $\exp(-2a^2/W^2) \approx 3.35 \times 10^{-4}$, of the beam power escapes on each pass [see (3.1-16)], the remainder being reflected (or absorbed in the mirror). Higher-order transverse modes suffer greater losses since they have greater spatial extent in the transverse plane.

When the mirror radius a is smaller than $2W$, the losses are greater. However, the Gaussian and Hermite–Gaussian beams no longer provide good approximations for the resonator modes. The problem of determining the modes of a spherical-mirror resonator with finite-size mirrors is difficult. A wave is a mode if it retraces its amplitude

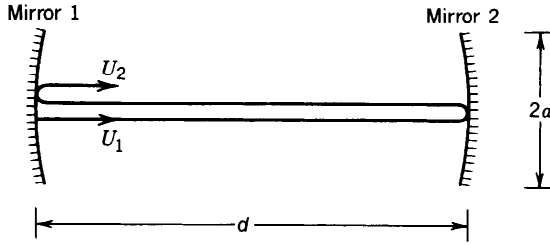


Figure 9.2-10 Propagation of a wave through a spherical-mirror resonator. The complex amplitude $U_1(x, y)$ corresponds to a mode if it reproduces itself after a round trip, i.e., if $U_2(x, y) = \mu U_1(x, y)$ and $\arg\{\mu\} = q2\pi$.

(to within a multiplicative constant) and reproduces its phase (to within an integer multiple of 2π) after completing a round trip through the resonator. One often-used method of determining the modes involves following a wave repeatedly as it bounces through the resonator, thereby determining its amplitude and phase, much as we determined the position and inclination of a ray bouncing within a resonator. After many round trips this process converges to one of the modes.

If $U_1(x, y)$ is the complex amplitude of a wave immediately to the right of mirror 1 in Fig. 9.2-10, and if $U_2(x, y)$ is the complex amplitude after one round trip of travel through the resonator, then $U_1(x, y)$ is a mode provided that $U_2(x, y) = \mu U_1(x, y)$ and $\arg\{\mu\}$ is an integer multiple of 2π (i.e., μ is real and positive). After a single round trip, the mode intensity is attenuated by the factor μ^2 , and the phase is reproduced. The methods of Fourier optics (Chap. 4) may be used to determine $U_2(x, y)$ from $U_1(x, y)$. These quantities may be regarded as the output and input, respectively, of a linear system (see Appendix B) characterized by an impulse-response function $h(x, y; x', y')$,

$$U_2(x, y) = \int_{-\infty}^{\infty} \int_{-\infty}^{\infty} h(x, y; x', y') U_1(x', y') dx' dy'.$$

If the impulse-response function h is known, the modes can be determined by solving the eigenvalue problem described by the integral equation (see Appendix C)

$$\int_{-\infty}^{\infty} \int_{-\infty}^{\infty} h(x, y; x', y') U(x', y') dx' dy' = \mu U(x, y). \quad (9.2-29)$$

The solutions determine the eigenfunctions $U_{l,m}(x, y)$, and the eigenvalues $\mu_{l,m}$, labeled by the indices (l, m) . The modes are the eigenfunctions and the round-trip multiplicative factor is the eigenvalue. The squared magnitude $|\mu_{l,m}|^2$ is the round-trip intensity reduction factor for the (l, m) mode. Clearly, when the mirrors are infinite in size and the paraxial approximation is satisfied, the modes reduce to the family of Hermite–Gaussian beams discussed earlier.

It remains to determine $h(x, y; x', y')$ and to solve the integral equation (9.2-29). A single pass inside the resonator involves traveling a distance d , truncation by the mirror aperture, and reflection by the mirror. The remaining pass, needed to comprise a single round trip, is similar. The impulse-response function $h(x, y; x', y')$ can then be determined by application of the theory of Fresnel diffraction (Sec. 4.3B). In general, however, the modes and their associated losses can be determined only by numerically solving the integral equation (9.2-29). An iterative numerical solution begins with an initial guess U_1 , from which U_2 is computed and passed through the system one more round trip, and so on until the process converges.

This technique has been used to determine the losses associated with the various modes of a spherical-mirror resonator with circular apertures of radius a . The results

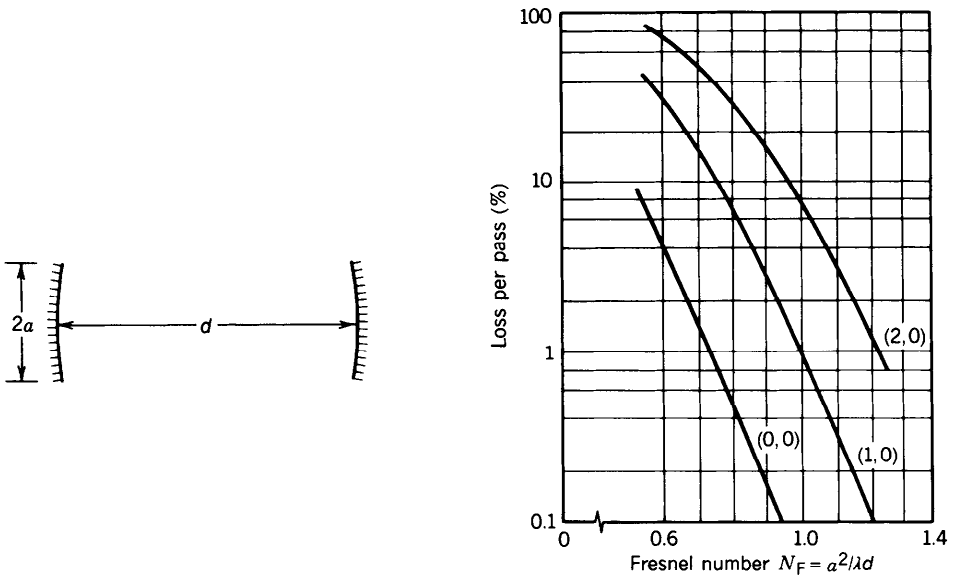


Figure 9.2-11 Percent diffraction loss per pass (half a round trip) in a symmetrical confocal resonator as a function of the Fresnel number $N_F = a^2 / \lambda d$ for the (0, 0), (1, 0), and (2, 0) modes. (Adapted from A. E. Siegman, *Lasers*, University Science Books, Mill Valley, CA, 1986.)

are illustrated in Fig. 9.2-11. For a symmetrical confocal resonator the loss is governed by a single parameter, the Fresnel number $N_F = a^2 / \lambda d$. This is because the Fresnel number governs Fresnel diffraction between the two mirrors, as discussed in Sec. 4.3B. For the symmetrical confocal resonator described by (9.2-20) and (9.2-21), the beam radius at the mirrors is $W = (\lambda d / \pi)^{1/2}$, so that $\lambda d = \pi W^2$, from which the Fresnel number is readily determined to be $N_F = a^2 / \pi W^2$. N_F is therefore proportional to the ratio a^2 / W^2 ; a higher Fresnel number corresponds to a smaller loss. From Fig. 9.2-11, for example, the loss per pass of the lowest-order mode $(l, m) = (0, 0)$ is about 0.1% when $N_F \approx 0.94$. This Fresnel number corresponds to $a / W = 1.72$. For a Gaussian beam of radius W , the percentage of power contained outside a circle of radius $a = 1.72W$ is $\exp(-2a^2 / W^2) \approx 0.27\%$. Higher-order modes suffer from greater losses because of their larger spatial extent.

READING LIST

Books on Resonators

- J. M. Vaughan, *The Fabry-Perot Interferometer*, Adam Hilger, Bristol, England, 1989.
Y. Anan'ev, *Résonateurs optiques et problème de divergence du rayonnement laser*, Mir, Moscow, Russian original 1979, French translation 1982.
L. A. Weinstein, *Open Resonators and Open Waveguides*, Golem, Boulder, CO, 1969.

Books on Lasers with Chapters on Resonators

See also the reading list in Chapter 13.

- A. Yariv, *Optical Electronics*, Holt, Rinehart and Winston, New York, 4th ed. 1991.
J. T. Verdeyen, *Laser Electronics*, Prentice-Hall, Englewood Cliffs, NJ, 2nd ed. 1989.
O. Svelto, *Principles of Lasers*, Plenum Press, New York, 3rd ed. 1989.
P. W. Milonni and J. H. Eberly, *Lasers*, Wiley, New York, 1988.

- J. Wilson and J. F. B. Hawkes, *Lasers: Principles and Applications*, Prentice-Hall, Englewood Cliffs, NJ, 1987.
- W. Witteman, *The Laser*, Springer-Verlag, New York, 1987.
- A. E. Siegman, *Lasers*, University Science Books, Mill Valley, CA, 1986.
- K. Shimoda, *Introduction to Laser Physics*, Springer-Verlag, New York, 2nd ed. 1986.
- A. E. Siegman, *An Introduction to Lasers and Masers*, McGraw-Hill, New York, 1971.
- A. Maitland and M. H. Dunn, *Laser Physics*, North-Holland, Amsterdam, 1969.

Articles

- A. E. Siegman, Unstable Optical Resonators, *Applied Optics*, vol. 13, pp. 353–367, 1974.
- H. Kogelnik and T. Li, Laser Beams and Resonators, *Applied Optics*, vol. 5, pp. 1550–1567, 1966 (published simultaneously in *Proceedings of the IEEE*, vol. 54, pp. 1312–1329, 1966).
- A. E. Siegman, Unstable Optical Resonators for Laser Applications, *Proceedings of the IEEE*, vol. 53, pp. 277–287, 1965.
- A. G. Fox and T. Li, Resonant Modes in a Maser Interferometer, *Bell System Technical Journal*, vol. 40, pp. 453–488, 1961.
- G. D. Boyd and J. P. Gordon, Confocal Multimode Resonator for Millimeter Through Optical Wavelength Masers, *Bell System Technical Journal*, vol. 40, pp. 489–508, 1961.

PROBLEMS

- 9.1-1 **Resonance Frequencies of a Resonator with an Etalon.** (a) Determine the spacing between adjacent resonance frequencies in a resonator constructed of two parallel planar mirrors separated by a distance $d = 15$ cm in air ($n = 1$).
(b) A transparent plate of thickness $d_1 = 2.5$ cm and refractive index $n = 1.5$ is placed inside the resonator and is tilted slightly to prevent light reflected from the plate from reaching the mirrors. Determine the spacing between the resonance frequencies of the resonator.
- 9.1-2 **Mirrorless Resonators.** Semiconductor lasers are often fabricated from crystals whose surfaces are cleaved along crystal planes. These surfaces act as reflectors and therefore serve as the resonator mirrors. The reflectance is given in (6.2-14). Consider a crystal with refractive index $n = 3.6$ placed in air ($n = 1$). The light reflects between two parallel surfaces separated by the distance $d = 0.2$ mm. Determine the spacing between resonance frequencies ν_F , the overall distributed loss coefficient α_r , the finesse \mathcal{F} , and the spectral width $\delta\nu$. Assume that the loss coefficient $\alpha_s = 1 \text{ cm}^{-1}$.
- 9.1-3 **Resonator Spectral Response.** The transmittance of a symmetrical Fabry–Perot resonator was measured by using light from a tunable monochromatic light source. The transmittance versus frequency exhibits periodic pulses of period 150 MHz, each of width (FWHM) 5 MHz. Assuming that the medium within the resonator mirrors is a gas with $n = 1$, determine the length and finesse of the resonator. Assuming that the only source of loss is associated with the mirrors, find their reflectances.
- 9.1-4 **Optical Decay Time.** What time does it take for the optical energy stored in a resonator of finesse $\mathcal{F} = 100$, length $d = 50$ cm, and refractive index $n = 1$, to decay to one-half of its initial value?
- 9.1-5 **Number of Modes.** Consider light of wavelength $\lambda_o = 1.06 \text{ }\mu\text{m}$ and spectral width $\Delta\nu = 120 \text{ GHz}$. How many modes have frequencies within this linewidth in the following resonators ($n = 1$):
(a) A one-dimensional resonator of length $d = 10 \text{ cm}$?
(b) A $10 \times 10 \text{ cm}^2$ two-dimensional resonator?
(c) A $10 \times 10 \times 10 \text{ cm}^3$ three-dimensional resonator?

- 9.2-1 **Stability of Spherical-Mirror Resonators.** (a) Can a resonator with two convex mirrors ever be stable?
 (b) Can a resonator with one convex and one concave mirror ever be stable?
- 9.2-2 **A Planar-Mirror Resonator Containing a Lens.** A lens of focal length f is placed inside a planar-mirror resonator constructed of two flat mirrors separated by a distance d . The lens is located at a distance $d/2$ from each of the mirrors.
 (a) Determine the ray-transfer matrix for a ray that begins at one of the mirrors and travels a round trip inside the resonator.
 (b) Determine the condition of stability of the resonator.
 (c) Under stable conditions sketch the Gaussian beam that fits this resonator.
- 9.2-3 **Self-Reproducing Rays.** Consider a symmetrical resonator using two concave mirrors of radii R separated by a distance $d = 3|R|/2$. After how many round trips through the resonator will a ray retrace its path?
- 9.2-4 **Ray Position in Unstable Resonators.** Show that for an unstable resonator the ray position after m round trips is given by $y_m = \alpha_1 h_1^m + \alpha_2 h_2^m$, where α_1 and α_2 are constants, and where $h_1 = b + (b^2 - 1)^{1/2}$ and $h_2 = b - (b^2 - 1)^{1/2}$, and $b = 2(1 + d/R_1)(1 + d/R_2) - 1$. *Hint:* Use the results in Sec. 1.4D.
- 9.2-5 **Ray Position in Unstable Symmetrical Resonators.** Verify that a symmetrical resonator using two concave mirrors of radii $R = -30$ cm separated by a distance $d = 65$ cm is unstable. Find the position y_1 of a ray that begins at one of the mirrors at position $y_0 = 0$ with an angle $\theta_0 = 0.1^\circ$ after one round trip. If the mirrors have 5-cm-diameter apertures, after how many round trips does the ray leave the resonator? Write a computer program to plot y_m , $m = 2, 3, \dots$, for $d = 50$ cm and $d = 65$ cm. You may use the results of Problem 9.2-4.
- 9.2-6 **Gaussian-Beam Standing Waves.** Consider a wave formed by the sum of two identical Gaussian beams propagating in the $+z$ and $-z$ directions. Show that the result is a standing wave. Using the boundary conditions at two ideal mirrors placed such that they coincide with the wavefronts, derive the resonance frequencies (9.2-24).
- 9.2-7 **Gaussian Beam in a Symmetrical Confocal Resonator.** A symmetrical confocal resonator with mirror spacing $d = 16$ cm, mirror reflectances 0.995, and $n = 1$ is used in a laser operating at $\lambda_0 = 1 \mu\text{m}$.
 (a) Find the radii of curvature of the mirrors.
 (b) Find the waist of the $(0, 0)$ (Gaussian) mode.
 (c) Sketch the intensity distribution of the $(1, 0)$ mode at one of the mirrors and determine the distance between its two peaks.
 (d) Determine the resonance frequencies of the $(0, 0)$ and $(1, 0)$ modes.
 (e) Assuming that the only losses result from imperfect mirror reflectances, determine the resonator loss coefficient α_r .
- 9.2-8 **Diffraction Loss.** The percent diffraction loss per pass for the different low-order modes of a symmetrical confocal resonator is given in Fig. 9.2-11, as a function of the Fresnel number $N_F = a^2/\lambda d$ (where d is the mirror spacing and a is the radius of the mirror aperture). Using the parameters provided in Problem 9.2-7, determine the mirror radius for which the loss per pass of the $(1, 0)$ mode is 1%.